RESEARCH ARTICLE

WILEY

Geomorphological response to system-scale river rehabilitation I: Sediment supply from a reconnected tributary

Baptiste Marteau[1,2] | Chris Gibbins[1,3] | Damià Vericat[4,5] | Ramon J. Batalla[4,6,7]

[1]Northern Rivers Institute (NRI), Geosciences, University of Aberdeen, Aberdeen, UK

[2]Université de Lyon, CNRS, UMR 5600 – Environnement-Ville-Société (EVS), ENS Lyon, Lyon, France

[3]School of Environmental and Geographical Sciences, University of Nottingham Malaysia, Semenyih, Malaysia

[4]Fluvial Dynamics Research Group (RIUS), University of Lleida, Lleida, Spain

[5]Forest Science and Technology Centre of Catalonia (CTFC), Solsona, Spain

[6]Catalan Institute for Water Research (ICRA), Girona, Spain

[7]Faculty of Forest Sciences and Natural Resources, Universidad Austral de Chile, Valdivia, Chile

Correspondence
Baptiste Marteau, Université de Lyon, CNRS UMR 5600 – Environnement-Ville-Société (EVS), ENS Lyon, Lyon, France.
Email: baptiste.marteau@ens-lyon.fr

Abstract

This paper is the first of a pair that report the findings of a river rehabilitation project centred on the reconnection of a formerly diverted headwater tributary (Ben Gill) to its main-stem river (the River Ehen). The present paper describes the geomorphic evolution of the tributary in the 2 years following its reconnection, with a particular focus on assessing the volumes of sediment now being supplied to the main-stem Ehen. Structure-from-Motion photogrammetry was used to produce Digital Elevation Models (DEMs) of the newly connected tributary, with successive DEMs compared to assess topographic changes in the channel and quantify volumes of material exported. 3D errors in the DEMs were small relative to the scour and fill observed in the channel (error 0.016–0.056 m compared to up to 1.7 m vertical change between consecutive surveys). Erosion was the dominant process in the tributary channel, though this varied spatially and temporally. Over the 2-year period, an estimated minimum of 384 m^3 of coarse sediment was exported from Ben Gill and delivered to the confluence zone, where a new bar feature developed as a result. This estimate is twice as high as earlier ones. Analysis of the growth of this bar suggested that much of the material supplied by Ben Gill remains here temporarily, with onward conveyance constrained by the competence of the regulated main-stem. The work shows that, thanks to the reconnection, this small (0.55 km^2) ephemeral tributary (flowing for only around 20% of the time) has become a key source of sediment for the main-stem Ehen. The second in the pair of papers focuses on the geomorphic responses of the main-stem to this renewed supply of sediment.

KEYWORDS

catchment scale, connectivity, river Ehen, river rehabilitation, sediment transport, SfM photogrammetry

1 | INTRODUCTION

Catchment-scale connectivity is recognised as important for the healthy functioning of fluvial ecosystems (Fryirs, 2013; Fuller & Death, 2018; Wohl, 2017), with sediment connectivity considered an important component of this (Bracken, Turnbull, Wainwright, & Bogaart, 2015). Disconnection of rivers from their sources of water and sediment (i.e., the loss of connectivity) affects their transport capacity and sediment supply and, consequently, sediment dynamics and loads in downstream river reaches. For instance, dams are capable of trapping virtually all of the coarse sediment transported by rivers (e.g., Batalla & Vericat, 2011; Tena, Batalla, & Vericat, 2012; Vericat,

Batalla, & Garcia, 2006; Williams & Wolman, 1984), and this disconnection has major implications for fluvial processes and conditions downstream (Gaeuman, 2012; Kondolf, 1997). Instream gravel mining (Kondolf, 1994) and changes in land use and land cover also alter sediment supply (e.g., afforestation, Buendía et al., 2016), with the latter influencing transport capacity due to changes in runoff. Small scale flow regulation, including that resulting from weirs and the diversion or disconnection of tributaries, can also affect sediment dynamics in main-stem rivers (Quinlan, Gibbins, Batalla, & Vericat, 2015).

The consequences of disconnection for fluvial dynamics in downstream river reaches have been studied extensively, although less so for small dams (e.g., "run-of-river" impoundments, Csiki & Rhoads, 2010), and depend on factors that include dam operation, the magnitude of changes in flow and flood regimes, and channel characteristics (Kondolf, 1997). Disconnection results in adjustments to geomorphic conditions that include incision, armouring, vegetation encroachment and simplification of channel morphology, and such adjustments have been observed in regulated rivers around the world (e.g., Batalla & Vericat, 2011; Church, 1995; Kondolf, 1997; Pitlick & Wilcock, 2001; Sear, 1995). In addition, aggradation can be observed in rivers where flow regimes have been reduced to the point that they can no longer carry the sediment supplied by tributaries (Kondolf, Podolak, & Grantham, 2012), or when this sediment is coarser than that normally transported by the receiving system (Ferguson, Cudden, Hoey, & Rice, 2006). In such cases, the role of tributaries in downstream recovery is crucial from both sedimentary (Tena et al., 2012) and hydrological (Piqué, Batalla, & Sabater, 2016) perspectives. The supply of sediments from such tributaries can also increase habitat heterogeneity (Rice, 2017), and so may be ecologically important.

Consequences of the physical alteration of rivers, and particularly sediment depletion, extend across all aspects of their ecology (e.g., invertebrates, Boon, 1988; fish, Allan & Castillo, 2007; algae, Ponsatí et al., 2015) including processes and feedbacks (length of the food-chain, Wootton, Parker, & Power, 1996; food-web transfer of energy, Parker & Power, 1997; nutrient processing, Abril et al., 2015). Recognition of the problems of sediment starvation and fluvial adjustment has led to widespread river restoration or rehabilitation efforts. There are two ways that sedimentary activity can be re-instated as part of such efforts: (a) by feeding the river artificially (i.e., gravel augmentation), or (b) by restoring connectivity pathways (e.g., sediment pass-through and/or dam removal, Foley et al., 2017; Espa et al., 2019). Gravel augmentation has become a widespread and common practice to mitigate the effects of reductions or total cessation of sediment supply (Brousse et al., 2019; Gaeuman, 2012; Habersack & Piégay, 2008; Kondolf et al., 2014), and is most often used in upland rivers where coarse sediment is a critical component of the habitat of economically and culturally important salmonid fish. However due to the high cost of such artificial augmentation, and the fact that benefits may be short-lived (Harvey, McBain, Reiser, Rempel, & Sklar, 2005), other options are needed. A high sediment conveyance can be achieved when sediment connectivity is high (e.g., Fuller, Large, Charlton, Heritage, & Milan, 2003; López-Tarazón, Batalla, Vericat, & Francke, 2009). Restoring connectivity pathways with natural sources

of sediment, when possible, may therefore represent a more suitable alternative to artificial augmentation. However, other than the increasing number of dam removal initiatives, examples of projects reconnecting affected channels to sediment source areas remain few.

The River Ehen (NW England) has suffered from reduced sediment supply and flow competence due to the construction of a weir and the diversion of a tributary (Quinlan, Gibbins, Batalla, & Vericat, 2015). The result of these changes is that riverbed conditions have become suboptimum for the freshwater pearl mussel (*Margaritifera margaritifera* L.), an endangered species threatened throughout its Holarctic range (Young, Cosgrove, & Hastie, 2001) that is present in the Ehen (the river supports the largest population remaining in England, Killeen, 2006; O'Leary, 2013). Improving the suitability of bed conditions for mussels is essential for their conservation (Quinlan et al., 2015), both at the reach and catchment scales (Gumpinger, Hauer, & Scheder, 2015). Accordingly, over the last decade the River Ehen has benefitted from a catchment-wide restoration scheme, which most notably includes the reconnection of a headwater tributary, Ben Gill. This tributary is recognised as being an important source of fine and coarse sediment to the main-stem (Marteau, Batalla, Vericat, & Gibbins, 2017, 2018), so the aim of the reconnection has been to reinstate more natural (dynamic) fluvial processes in the Ehen and counteract the ongoing degradation of physical habitat that resulted from flow regulation and tributary diversion.

The overarching goal of the work described in the present and its companion paper (Marteau, Gibbins, Vericat, & Batalla, 2020) was to understand how reconnecting rivers to their sources areas, as an alternative to artificial gravel augmentation at a given point in time and space, influences fluvial processes and geomorphic conditions. The present paper reports on the geomorphic evolution of the tributary following its reconnection to the Ehen, as well as the volumes of coarse material eroded from its channel and delivered to the main-stem. Its specific objectives are: (a) to quantify the volumes and temporal dynamics of coarse sediment delivered from the reconnected sub-catchment, and (b) to assess the development of a newly formed confluence bar and its role in mediating the interaction between this sub-catchment and its main-stem. Marteau et al. (2020) present information on the geomorphic responses of the river Ehen to this renewed delivery of coarse material.

2 | STUDY CONTEXT AND AREA

2.1 | The catchment and the river

The Ehen is a 24.6 km long river flowing south-westwards from Ennerdale Water to the Irish Sea (Figure 1a,b). Ennerdale Water and the upstream River Liza drain a 44.5 km² catchment. The lake is a natural glacial relic and an important local supply of drinking water. Actions were taken in the past to improve its storage capacity, including the construction of a 1.3-m high weir (1902) and the diversion of Ben Gill (the main headwater tributary of the Ehen) to the lake (1970s). Ben Gill is a first order ephemeral tributary, with a small
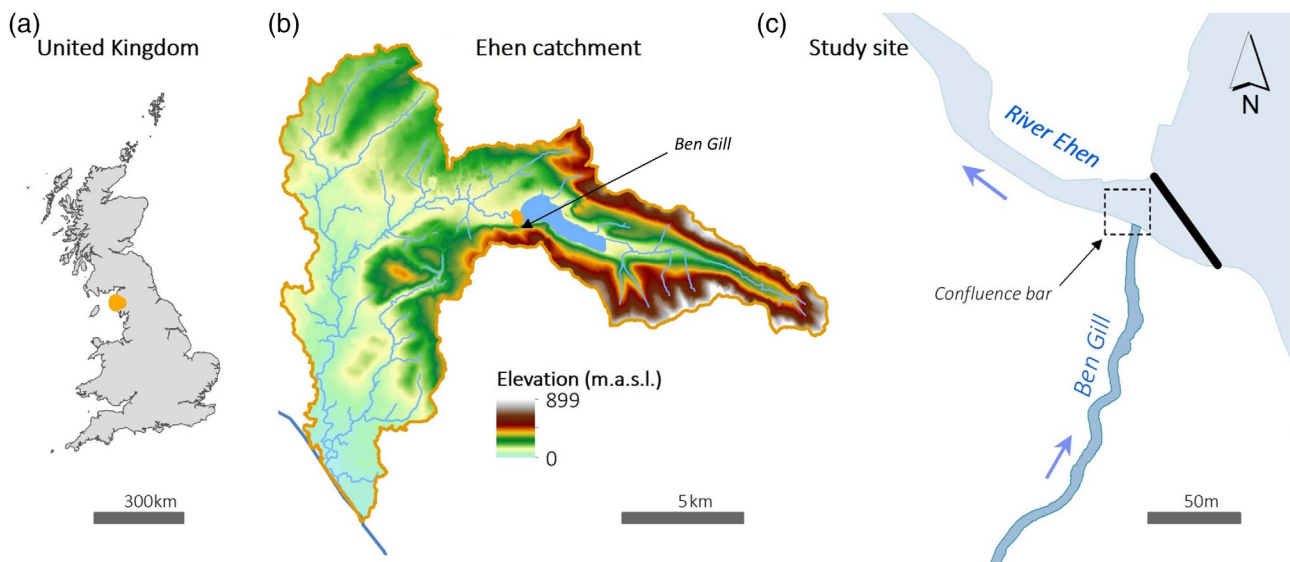
FIGURE 1 Location of the river Ehen study area. (a) Within the UK. (b) Digital Elevation Model of the Ehen catchment. (c) The study site, showing the upper Ehen, Ben Gill and the confluence area. The weir at the lake outlet is shown as a black line [Colour figure can be viewed at wileyonlinelibrary.com]

(0.55 km²) and steep catchment (mean catchment slope: 25%). It flows for <25% of the time and is very responsive to local rainfall events (Marteau et al., 2018; Quinlan, 2014). The diversion involved the lowermost 300 m of Ben Gill channel being filled, with water redirected to the lake via an underground culvert. The upper part of the stream (*c.* 85% of its total length) was left untouched, and sediment delivered to the culvert entrance was retained by a grill and removed periodically and used by local people. In the 50 years since its diversion, Ben Gill has been unable to deliver its water and sediment loads to the main-stem Ehen.

2.2 | The Ehen restoration project

The presence of mature pearl mussels in the river Ehen (individuals more than 100 years old, Killeen & Oliver, 1997) indicates that habitat conditions must have been adequate for survival and reproduction prior to the diversion of Ben Gill. However, the current lack of juveniles (indicating a lack of recruitment) implies that this is not the case anymore (Killeen & Moorkens, 2013; O'Leary, 2013) and can be at least partly attributed to shortage of suitably coarse sediment in the Ehen and lack of geomorphic activity that have resulted in a heavily paved bed (Brown, Butterill, & Bayliss, 2008; Quinlan, 2014; Quinlan, Gibbins, Batalla, & Vericat, 2015).

Despite the relatively small size of Ben Gill catchment compared to that of the Ehen, most of the geomorphic changes in the upper part of the river can be attributed to the disconnection of this tributary. Although changes in land-use and management practices have been observed upstream from Ennerdale Water (deforestation, mineral extraction, increase in grazing; O'Leary, 2013) the potential consequences of these for the Ehen have been smothered by the presence of the lake which acts as an efficient sediment trap from which virtually no coarse material escapes (Brown et al., 2008). During drawdown

periods, gravel deposits are evident along the shores of the lake (Brown et al., 2008) and near the weir (pers. observations), from which there may have been some limited extraction in the 1920–1940s (Alvarez-Codesal & Sweeting, 2015). The engineering works related to different phases of construction and enhancement of the weir, including the addition of a fish pass, have contributed to the sediment clearing and channel widening in the immediate vicinity of the weir (Alvarez-Codesal & Sweeting, 2015; Brown et al., 2008), although geomorphic conditions further downstream cannot be attributed only to these local actions. Moreover, the age gap identified in the pearl mussel population of the upper Ehen coincides with the disconnection of the headwater tributary (Killeen, 2006). Geomorphic alterations are dampened once the next downstream tributary, Croasdale Beck, provides an undisturbed supply of coarse material (Gibbins et al., 2004). All evidence at hand therefore points to the importance of Ben Gill for the geomorphic activity of the upper Ehen. Concerns over the deterioration of geomorphic conditions in this part of the river created the impetus for the reconnection of Ben Gill.

To reconnect Ben Gill catchment to the Ehen, the lower part of the tributary channel (i.e., that below the diversion culvert) was re-dug so as to follow its original (pre-diversion) course. This work took place in late summer 2014. The new channel was 5 m wide and 0.5 m deep on average, and designed to convey an estimated 100-year flood (estimated as 80 m³ s⁻¹ United Utilities, 2012). This re-engineered section cuts across an alluvial fan and is approximately 300 m long, with an average slope of 9.4%. It was lined with cobble-size material (between 20 and 250 mm *b*-axis) with a few larger boulders along the sides (see fig. 1C in Marteau, Vericat, Gibbins, Batalla, & Green, 2017 and Figure S1). The new channel was dug sequentially from top to bottom, with the final section (i.e., where it meets the Ehen, *c.* 25 m downstream from the weir, Figure 1c) excavated on October 3, 2014. Completion of this final section effectively reconnected Ben Gill to the Ehen, with the first flows occurring the following day. Since then,

the new channel has been subject to processes driven by rainfall and sediment supplied by the upstream contributing catchment, and is potentially capable of eroding through the alluvial fan and delivering water and sediment into the Ehen.

Ongoing monitoring since the reconnection has shown that its goals are beginning to be achieved: large volumes of coarse material are now being delivered to the Ehen (Marteau, Vericat, et al., 2017). However, the tributary is also delivering large volumes of fine material, and has become the main driver of fine sediment dynamics in the Ehen (Marteau, Batalla, et al., 2017). The effects of this on suspended sediment concentrations and in-channel storage in the Ehen are controlled by the degree of asynchronicity between flows in the main-stem and those in the ephemeral tributary (Marteau et al., 2018).

Although there are no data on the rates of coarse material export from Ben Gill prior to its diversion, several pieces of evidence exist to help build a sense of its geomorphic activity. Most notably, aerial images from 1970 (before its diversion) show an extensive depositional bar at the confluence (Figure 2). Since the diversion, sediment over-spilling the culvert grid has been periodically removed (United Utilities, 2012). Based on these lines of evidence, preliminary studies estimated that an average of 100 m^3 of coarse material was prevented from discharging in the Ehen every year as a result of the diversion of Ben Gill (Brown et al., 2008; United Utilities, 2012). Ben Gill bed material is generally coarser than that found in the Ehen (median particle size, that is, D_{50} is 77 mm in Ben Gill, and between 36 and 55 in the Ehen, while larger sizes, for example, D_{84}, reaches 149 mm in Ben Gill, and between 59 and 103 in the Ehen; Quinlan, 2014, see Figure 2).

This paper presents information on changes in Ben Gill and on material being delivered to the Ehen in the first 2 years following the reconnection. Given the 40 years of water being diverted to the lake, the removal of sediment from the grid and the infilling and associated terrestrialisation of the original lower part of Gen Gill channel, the changes reported here have to be considered as representing the early adjustment phase. Rates of processes, sediment delivery and sediment characteristics will likely change over time as the system adjusts to its new state.

3 | METHODS

3.1 | Characterisation of flows in Ben Gill

Because Ben Gill is not gauged, information on flow conditions was collated from different sources, including field notes and observations. In June 2015 a time-lapse camera was installed facing the confluence with the Ehen. Flow events in Ben Gill were characterised qualitatively (i.e., classification into flowing or not flowing) using the images acquired by the camera at 1 hr interval for the duration of the present study; data are used as a proxy for discharge in Ben Gill. These images were used in a previous study to assess the implications of asynchronicity of flows in the Ehen and those in the tributary for fine sediment transport and storage (Marteau et al., 2018).

3.2 | Estimating bed material supply from topographic surveys

Ben Gill and the confluence bar were surveyed and topographic changes between successive surveys computed separately for the two features. These surveys are used to provide insights into the minimum volume of material entering in the main-stem (the net balance of
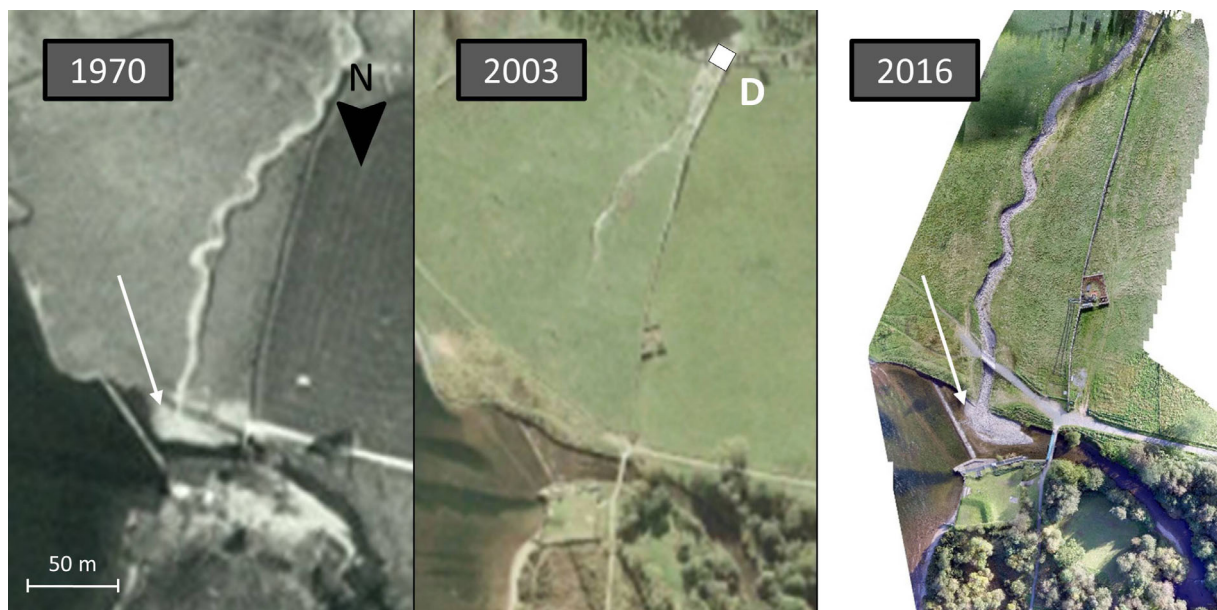
FIGURE 2 Aerial photos of the confluence of Ben Gill with the river Ehen, at the outlet of Ennerdale Water. Flow direction in the main-stem Ehen is from left to right. Arrow shows confluence bar. White square (D) on 2003 photograph shows location of the diverting grid. (Credit: 1970, Environment Agency [Penrith]; 2003, Google Maps; 2016, Jason Hagon on the account of the University of Aberdeen) [Colour figure can be viewed at wileyonlinelibrary.com]

sediment in the active channel of Ben Gill) and the role in passive transient storage played by the confluence bar, respectively.

Topographic point clouds and orthophotomaps for each survey (*n* = 8) were obtained using Structure-from-Motion and Multi-View Stereo photogrammetry (hereafter SfM), based on digital images collected from an Unmanned Aerial Vehicle (UAV). Digital Elevation Models (DEMs) were produced from 3D point-clouds, errors of DEMs were assessed independently and, finally, successive DEMs were compared (i.e., DEMs of Difference; DoDs) to monitor topographic changes and quantify net volumes of change taking into account potential uncertainties. Specific details of the workflow used to acquire and process SfM data can be found in Marteau, Vericat, et al. (2017) based on the analyses of the first three flights of the nine presented in the current paper. The workflow is represented schematically in Figure 4 of that paper. A summary of the main steps is given below.

3.2.1 | Data acquisition

A total of 196 fixed Ground Control Points (GCPs) were installed around the 300-m long channel of Ben Gill and surveyed with a Leica Viva® GNSS (Leica Geosystems) differential rtk-GPS. The 3D quality of the coordinates varied between 0.009 and 0.024 m. Flights were undertaken along three lines (both banks, then along the channel centreline) to yield appropriate overlap. More than 1,000 images were captured per survey. Surveys were conducted between October 2014 and October 2016 (Figure 3). Flight altitude remained between 10 and 20 m above ground, which was optimum given the characteristics of the equipment used (Marteau, Vericat, et al., 2017).

3.2.2 | Photogrammetry

Aerial pictures were processed using AgiSoft® PhotoScan Professional (Version 1.2.6) (AgiSoft LLC, 2015). Poor quality images from each survey were removed, based on (a) blurriness (b) over or under exposure to light, (c) graininess due to high ISO values, (d) the obstruction of features of interest (e.g., due to legs of the UAV) and (e) avoiding unnecessary overlap between images (i.e., when the UAV was static). The remaining images (<500 per flight) were aligned, with the centre of the GCPs identified and adjusted manually.

3.2.3 | Error analysis

The assessment of model accuracy was based on information obtained from the GCPs (as per Brasington, Rumsby, & McVey, 2000). This involved using some GCPs as markers (i.e., to georeference and register the models, here 131 GCPs) and the remainder as "check points" (ChP; to assess accuracy and precision of the models, here 65 GCPs). Registration error was calculated as the mean distance between the real location of markers and their projection in the georeferenced model (i.e., residuals). Accuracy was determined as the mean distance of the real location of the ChPs to their projection in the georeferenced model (i.e., residual), while precision was provided by the standard deviation of the residuals. Mean relative error is the true signed average distance of elevation residuals (i.e., z only). Here, instead of selecting a proportion of GCPs as ChP in a static manner, a bootstrapping algorithm was used to run this random selection 1,000 times, generating a value of registration error, precision and accuracy
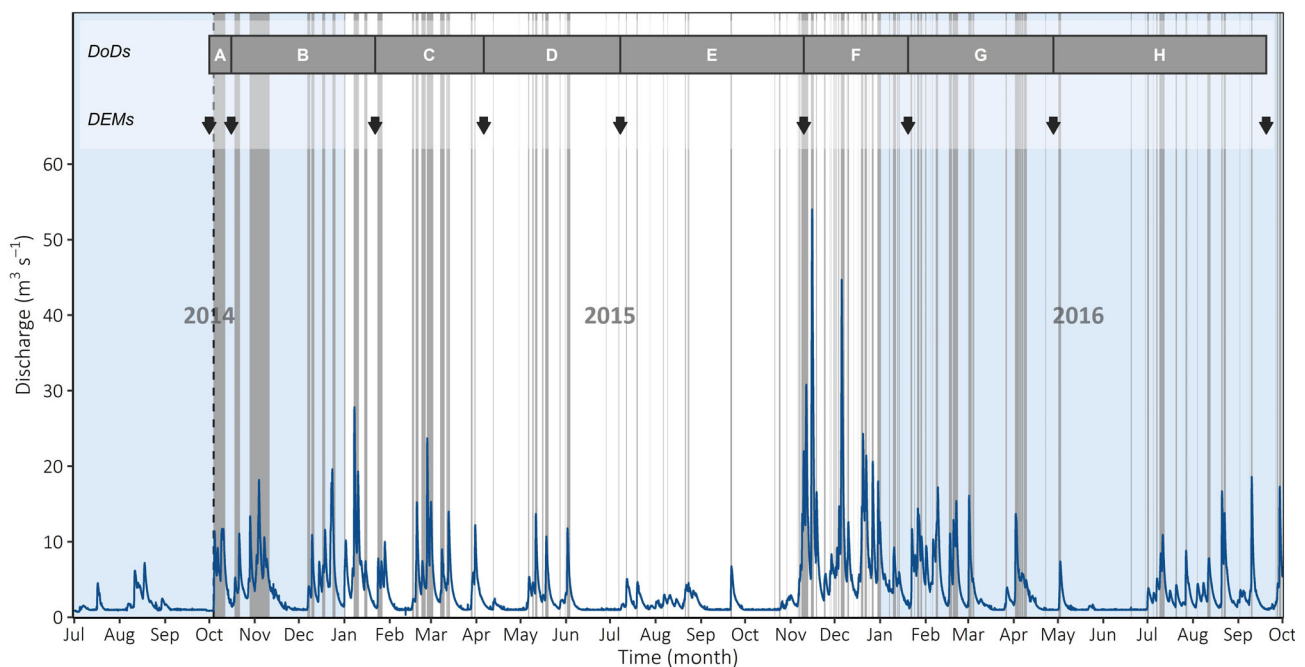
FIGURE 3 Hydrograph of the river Ehen over the study period (from Bleach Green gauging station), indicating key aspects of the study. Vertical grey bars show times when Ben Gill was flowing. Arrows show times of aerial surveys used to produce DEMs, and grey bars with letters refer to the time periods captured by DoDs produced from successive DEMs. DEM, Digital Elevation Model [Colour figure can be viewed at wileyonlinelibrary.com]

for each GCP. Model precision was used to determine a minimum level of detection (minLoD, Brasington, Langham, & Rumsby, 2003), by calculating the spatial distribution of *t*-scores (Lane, Westaway, & Hicks, 2003) which defines the probability of the change observed in each cell to be "certain" (confidence interval [CI] used here was 80%), as well as defining uncertainty bounds to gross and net volume estimates. MinLoDs were used to compute thresholded DoDs. Recent work by Anderson (2019) has highlighted the potential issues related to the use of thresholded DoDs when estimating net volumes of topographic changes, and these are discussed below.

3.2.4 | Outputs

The photogrammetry software generated aerial orthophotos in addition to 3D point-clouds. These were used complementarily. Dense point-clouds were decimated using ToPCAT (Brasington, Vericat, & Rychkov, 2012) to generate regularised point-clouds representing the minimum observation within a 0.05 by 0.05 m grid cells (ToPCAT is available from the GCD software, see http://gcd.riverscapes.xyz/). The minimum observations within these regular cells were considered the ground elevation. Triangulated Irregular Networks (TINs) were computed from these, before the creation of DEMs (at 0.05 m cell size). Orthophotos (at 0.025 m resolution) were used for image classification in order to differentiate vegetation from the riverbed (potentially wrongly interpreted as topographic changes due to episodes of growth and decay). Thresholded topographic changes were calculated for every successive DEM by the production of DoDs taking into account only changes considered certain at the 80% CI (i.e., changes above the minLoD), and uncertainty bounds were calculated from the spatial distribution of *t*-scores following Wheaton, Brasington, Darby, and Sear (2010). Changes below the minLoD were considered uncertain and not included in the computation of topographic changes. A total of seven DoDs provided data on the volumes of erosion and deposition in the channel over the study period (Figure 3), as well as an estimate of the minimum volume of sediment exported from the channel between successive surveys (net change). Similar information was computed for the deposition bar developing at the confluence with the Ehen, although some specific details needed to be considered here.

Application of photogrammetry remains challenging for submerged areas (Lane, 2000; Westaway, Lane, & Hicks, 2000). The ephemeral nature of Ben Gill rendered survey and analysis of this channel straightforward, as all flights were undertaken when it was dry. However, modelling topography of the confluence bar was constrained by water surface elevation in the Ehen and the water turbulence over the bar produced by the weir immediately upstream (such factors were discussed by Woodget, Carbonneau, Visser, & Maddock, 2014). Using the orthophotos of the confluence zone, submerged areas were identified and DEMs corrected following the procedure of Westaway, Lane, and Hicks (2001) and Woodget et al. (2014). The bed topography for submerged areas was corrected by the refractive index of clear water (1.34, see previous references)

applied to water depth. DEM error also increases with depth (Woodget et al., 2014), so values of model accuracy were adjusted accordingly. In the absence of field data to create an empirical model of error for submerged areas, the level of thresholding was multiplied by 2 in shallow areas (>10 cm) and 4 in deeper areas, which can be considered as being conservative relative to other studies (e.g., Westaway et al., 2001; Woodget et al., 2014). Areas of high surface turbulence were excluded altogether. As a consequence, one of the surveys (November 2015) had to be removed from the analysis because of limited bar exposure and high water turbulence.

UAV flights were undertaken on eight dates following the reconnection of Ben Gill. The initial plan was to undertake a pre-reconnection (baseline) aerial survey of the whole of the new channel as soon as all the engineering work was completed, and the machinery and related excavation equipment had been removed. This survey was scheduled for the first day after the opening. However, heavy rains and high flow in the channel prevented this survey going ahead. Therefore, to produce a "time zero *or initial*" DEM of the channel that could act as the reference (i.e., before any water was conveyed through it), topographic survey data collected by engineering contractors (those constructing the new channel) were used. This survey used an rtk-GPS and was based on 37 cross-sections along the 300-m long channel (i.e., average spacing of 8.1 m).

This baseline was used for assessment of cross-sectional topographic change over the short period between completion of the channel engineering works and the first aerial survey. For this, each point of each cross-section of the initial GPS survey was intersected with the first SfM-derived DEM (October 2014). Elevation of the SfM-derived DEM was extracted for each of these cross-sections and subsequently used to provide cross-sectional topography data. Thus, both sets of data share the same extension and density of points. Volumetric changes were calculated following Brewer and Passmore (2002), with difference in cross-sectional channel planform area divided between positive (elevation gain) and negative (elevation loss) difference (i.e., deposition and erosion respectively). Volumetric changes for each segment were calculated between cross-sections assuming that the change in area at a cross-section is representative over the half-distance to each adjacent cross-section:

$$\Delta V_{i[e;d]} = L_{(i,i+1)} \cdot \frac{\left(\Delta A_{i[e;d]} + \Delta A_{i+1[e;d]}\right)}{2}, \tag{1}$$

where $\Delta V_{i[e;d]}$ is the volume of change (m^3) associated with cross section *i*, for erosion (*e*) and deposition (*d*), $\Delta A_{i[e;d]}$ is the change in area at cross-section *i*, $\Delta A_{i+1[e;d]}$ is the change in area at the next upstream cross-section, and $L_{(i,i+1)}$ is the distance between the two cross-sections. Total volume of change (V_c) for a channel segment *a* was then calculated as:

$$V_{c(a)} = \sum \left[\Delta V_{a[e]} + \Delta V_{a[d]}\right]. \tag{2}$$

The sum of the volume of changes for each individual segment then represents the total volume of change of the channel (i.e., 37

segments). Uncertainties associated with this method are numerous (Arnaud et al., 2017), but while complete assessment of uncertainties is out of the scope of this paper, the error values produced are used to determine the confidence in estimates of geomorphic change in Ben Gill (as considered in Section 3.2.1).

In order to compare results for this initial period (period A, Figure 3) with successive SfM-derived DoDs, a threshold of minimum level of detection at the cross-sectional area of difference (minLoD^2) was applied as follows:

$$minLoD^2 = \sqrt{\varepsilon_{GPS}{}^2 + \varepsilon_{DEM}{}^2} \cdot \left(\frac{W_i}{p_i - 1}\right), \qquad (3)$$

where ε_{GPS} and ε_{DEM} are the potential errors associated with each survey considered here, W_i is the width of cross-section i, p_i is the number of points on cross-section i. The second part of the equation is used to take into account uncertainties related to the density of points.

No geomorphic feature existed at the confluence prior to the opening of Ben Gill channel. As no topographic survey of the confluence at the same time was available as a channel baseline, the volume of deposition was estimated using the SfM-derived point cloud from October 2014. Using CloudCompare® (Version 2.8.1), the volume of the newly formed gravel bar was estimated from a simulated plan surface for the original bed. This did not allow for proper estimation of errors but helped provide an estimate of the sediment export associated with this first period.

3.2.5 | Uncertainties in the estimates of topographic change

Anderson (2019) argued that estimates computed from thresholded DoDs potentially miss part of topographic changes by removing erosion and deposition that maybe of low intensity but considered uncertain, but which in fact are real changes. Most studies that use thresholding do so with a CI of 95%, which is known to be quite stringent and conservative (Wheaton et al., 2010). In our case, a CI of 80% was used instead. The alternative approach proposed by Anderson (2019) relies on the computation of systematic, spatially correlated and uncorrelated errors. Spatially correlated as well as uncorrelated errors are calculated from the comparison of successive DEMs in stable areas. In the case of our study, the only available "truly" stable area was a 10 m^2 path leading to and from the footbridge at the bottom of Ben Gill channel, where mean elevation differences were low (<0.03 m, Table S2). So, given the absence of large and spatially relevant stable areas, using the approach suggested by Anderson (2019) was not possible. Moreover, systematic errors, which represent an offset in elevation between successive topographic surveys, are in part caused by technical or methodological differences (Anderson, 2019; Lallias-Tacon, Liébault, & Piégay, 2014). In our case, systematic errors were limited by the use of a fixed network of GCPs which remained in place throughout the study. Because the exact same GCPs were used for all topographic models, systematic errors

are considered as being low. Consequently, the error propagation method, while based on the spatial distribution of *t-scores*, only considers what Anderson (2019) refers to as the random uncorrelated error. While the method used for Ben Gill has some limitations, local conditions meant that it was the most appropriate. Finally, the scale of topographic changes captured recorded (up to 1.7 m) greatly exceed the scale of model errors (<0.1 m). Thus, the widely used method of thresholding was used to improve confidence in gross and net estimates of change in Ben Gill. However, in order to lower the conservative nature of this approach, an 80% CI was used for the propagation of *t-scores* instead of the commonly used 95%.

3.3 | Characterisation of particle sizes on the confluence bar

Fluvial geomorphology has a long history of using remotely sensed data to characterise particle sizes. Recent advances have explored the possibility of using SfM-derived point cloud statistics to infer sediment sizes based on values of bed roughness derived from point clouds (Smith, 2014). However, as no single roughness metric is appropriate for application to all river types, site-specific correlations are needed (Brasington et al., 2012; Pearson, Smith, Klaar, & Brown, 2017; Woodget & Austrums, 2017). Three metrics were tested for their suitability to the Ehen confluence bar: roughness height *rh*, twice the local standard deviation of elevations ($2\sigma_z$), and detrended local standard deviation of elevations ($d\sigma_z$) (Pearson et al., 2017; Vázquez-Tarrío, Borgniet, Liébault, & Recking, 2017). To determine how these performed at representing particle size in Ben Gill, the *b*-axis of 100 particles were measured inside 1.5 × 1.5 m quadrats (Figure S2). Relevant particle size statistics (i.e., D_{16}, D_{50} and D_{84}) were compared to their counterparts obtained from each of the metrics using correlation analysis. This was repeated for eight quadrats over the April 2016 survey in sections of the channel with contrasting bed texture (i.e., different size range, degrees of sorting and imbrication).

The detrended standard deviation (Brasington et al., 2012), at a sub-grid level of 0.25 m, yielded the highest correlation coefficient (Figure 4). Correlation was best for median particle size (i.e., 0.75 at D_{50}), so this statistic was used primarily for further analysis of the temporal evolution of surface particle size across the confluence bar.
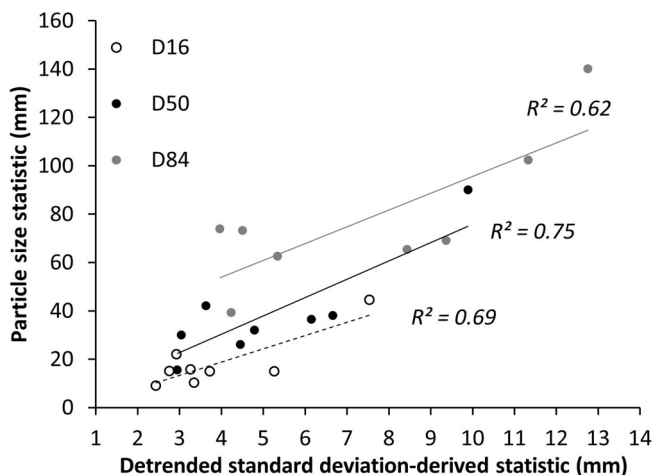
4 | RESULTS

4.1 | Hydrology

Flow in Ben Gill was recorded 19.4% of the time over the study period, with a total of 112 flow events recorded (Table 1). "Events" are considered as periods of flow lasting more than 2 hr (i.e., visible on at least two successive photographs). The first event happened the day after the reconnection and was the longest recorded (8.2 days) over the period. Typically, flows responded rapidly to local rainfall

events, and also recessed quickly; periods of flow lasted from just a few hours to a few days. The highest number of events was recorded in the 2 month period represented by DoD *F* (November 2015–January 2016), which corresponds to a period of high hydrological activity across the Ehen catchment as a whole (Figure 3). Activity in Ben Gill was lowest during the summer months of 2015 and 2016, when the channel was dry for extended periods.

4.2 | Observations in Ben Gill

4.2.1 | DEM errors and associated uncertainties

The 3D model accuracy of the successive point clouds was relatively high and constant (between 0.016 and 0.056 m, Table 2), allowing for the computation of high resolution DEMs and reliable estimates of topographic change. The accuracies of the DEMs are considered the same as those of the point clouds, and therefore errors associated with the generation of the DEM from the point cloud were not considered. Systematic errors could not be properly assessed, given the

FIGURE 4 Regressions between between field-measured particle size statistics (mm) and those estimated from detrended standard deviation of elevation (mm) at a sub-grid level of 0.25 m

limitations detailed earlier, but estimates from the gravel path yielded mean relative errors between 0.004 and 0.027 m (Table S2).

Uncertainties associated with the initial GPS survey (pre-reconnection) are unknown. However, due to the simplified structure of the channel at the time of survey (i.e., newly engineered, with no water reworking) and the quality of the GPS equipment used, an error of 0.1 m was assumed. By comparison, model accuracy of the first SfM-derived DEM (for October 2014) was 0.044 m (Table 2).

4.2.2 | Topographic changes

Ben Gill channel experienced marked erosion following the reconnection (Figure 5). Erosion was always the dominant process (between 66 and 91% of the volume of all change), with up to 1.7 m of scour observed in some places (e.g., for period F, Figure 5). Histograms at the bottom of Figure 5 show the distribution of the elevational changes and the associated volumes for each DoD. These histograms show that patterns of both erosion and deposition processes varied over time, with greater differences observed for erosion. The histogram for period D is bimodal for erosion, probably indicating two separate processes: a first "peak" driven by a large localised erosion (−1 m) (e.g., bank erosion), and a second "peak" (around −0.5 m) mainly representing small but frequent processes acting to reshape the channel bed. Positive topographic change (deposition) was mostly observed in the lower part of the channel, in the vicinity of the bridge. Deposition was generally of lower magnitude than erosion, although both covered similar plan areas. The mean thickness of topographic change was always higher for erosion than deposition. Period H saw the most spatially extensive topographic change, with only restricted parts of the channel experiencing neither erosion nor deposition.

4.2.3 | Bed material fluxes

The total estimated export of sediment from Ben Gill over the study period was 384 ± 64.9 m^3 (erosion = 679 ± 58.8 m^3, deposition = 295.3 ± 27.5 m^3, Table S1).

Bed material fluxes calculated from the DoDs for individual periods varied between 3.8 ± 39.0 and 108 ± 29.9 m^3 of sediment

TABLE 1 Summary table of flow statistics in Ben Gill associated with the DoDs

Model	Period	Number of flow events	Total duration of flow Day	Average duration of events in period Day
A	September 2014–October 2014	1	8.2	8.2
B	October 2014–January 2015	9	25.3	3.1
C	January 2015–April 2015	10	20.9	2.1
D	April 2015–July 2015	12	9.2	0.8
E	July 2015–November 2015	16	11.6	0.7
F	November 2015–January 2016	25	20.4	0.8
G	January 2016–April 2016	19	24.4	1.3
H	April 2016–October 2016	20	18.8	0.9

TABLE 2 Summary table of statistics of the topography models obtained from SfM photogrammetry

Model	Number of images	Average flight altitude m	Average pixel resolution cm²/pix	Average point density Point/m²	3D registration error m	3D model precision m	3D model accuracy m	Mean relative elevation error m
January 2015	361	15.6	0.0729	1,370	0.060	0.030	0.056	0.0011
April 2015	475	12.4	0.0454	2,210	0.039	0.017	0.035	−0.0000
July 2015	341	13.8	0.0590	1,690	0.039	0.017	0.035	0.0012
November 2015	399	12.4	0.0502	2000	0.073	0.048	0.047	−0.0051
January 2016	441	14.1	0.0590	1,690	0.029	0.014	0.026	0.0003
April 2016	526	19.7	0.1340	784	0.019	0.020	0.016	−0.0011
October 2016	367	15.1	0.0686	1,460	0.011	0.011	0.022	−0.0011

Note: The extension of these is limited to Ben Gill and its confluence to the Ehen.
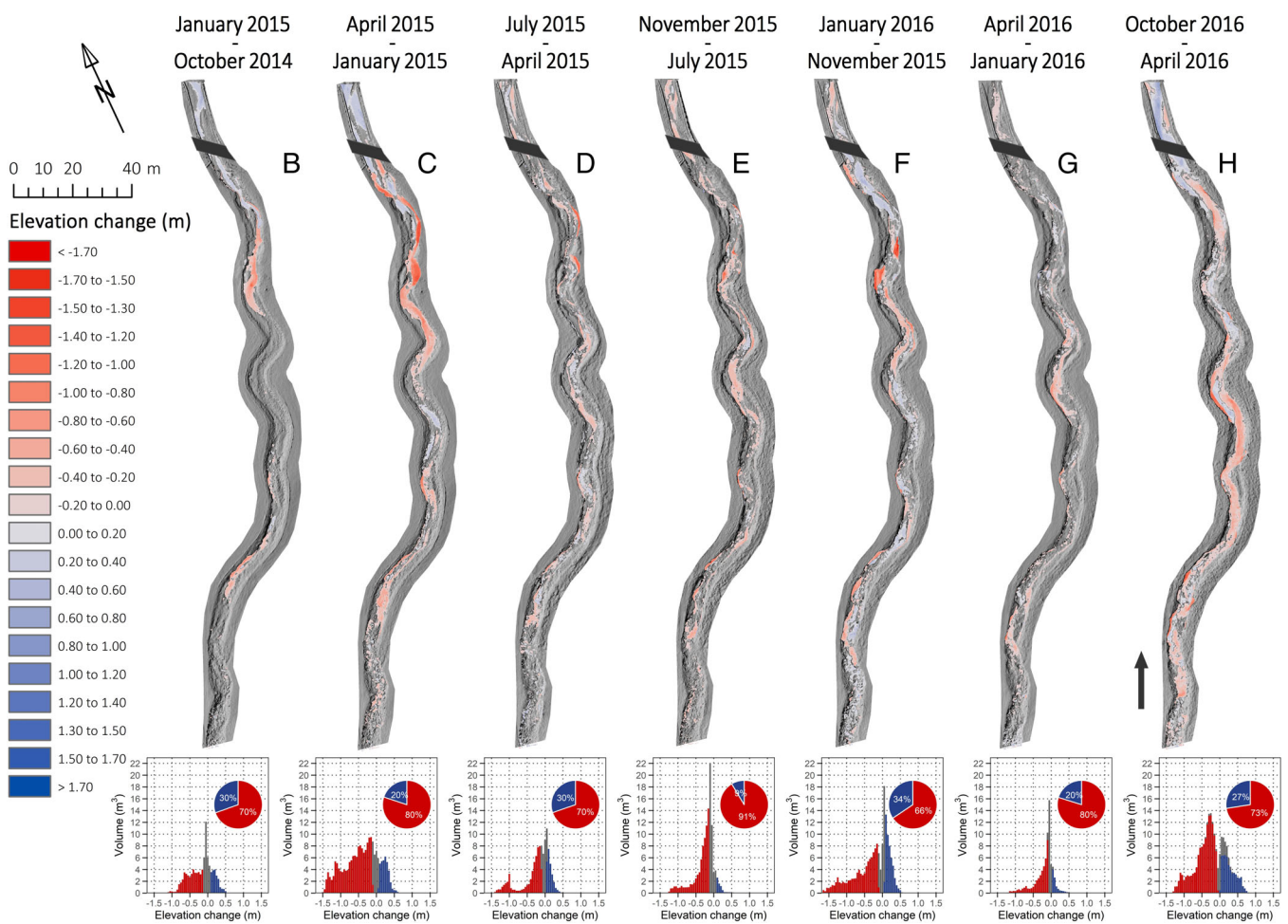
FIGURE 5 Topographic changes (DoDs) and associated histograms in Ben Gill channel. Letters refer to the different periods (see Figure 2). Colours in histograms show erosion (red), deposition (blue) and uncertain change (grey) [Colour figure can be viewed at wileyonlinelibrary.com]

and were lowest in period F (November 2015–January 2016) and greatest in period C (January–April 2015, Figure 6a). Period F still experienced appreciable topographic changes: the volumes of deposition were the highest recorded (83.0 ± 18.3 m³), indicating the active internal turnover of sediment despite the little export suggested by the net flux values. Topographic changes for period A

were assessed from cross-sections. The estimated sediment flux from Ben Gill for this period was *c.* 29.2 m³. Figure 6a shows the evolution of erosion, deposition and net change for the entire study period.

These values represent the minimum flux potentially transferred to the Ehen since material delivered from the upstream part of Ben

Gill catchment (i.e., upstream from the diversion grid) is not included in the (DoD-derived) calculations.

4.3 | Development and role of the confluence bar

4.3.1 | Topographic and volumetric changes

Topographic changes captured on the confluence bar were mainly depositional (Figure 7). Periods A and C experienced only deposition, with A being the largest episode of deposition experienced over a short period of time (c. 90 m^3 over 2 weeks). The highest proportion

of erosion (volumetrically, 66%) was observed over period G (−11.0 ± 6.3 m^3), which is also the only period where the erosion was dominant (Figure 6b). Important reworking of the bar occurred between July 2015 and January 2016 (EF, Figure 6b and Table S1) with the highest volume of erosion observed despite a large volume of deposition. Unfortunately, high water levels and turbulence at the confluence during the flight survey of November 2015 prevented the use of this DEM for geomorphic change detection (Figure 7). The total estimated storage of sediment at the confluence over the entire study period was 296 ± 28.6 m^3 (Erosion = 35.5 ± 8.1 m^3, Deposition = 331 ± 28.2 m^3).

The relative geomorphic changes in Ben Gill and the confluence bar show that not all material eroded from the channel was deposited at the
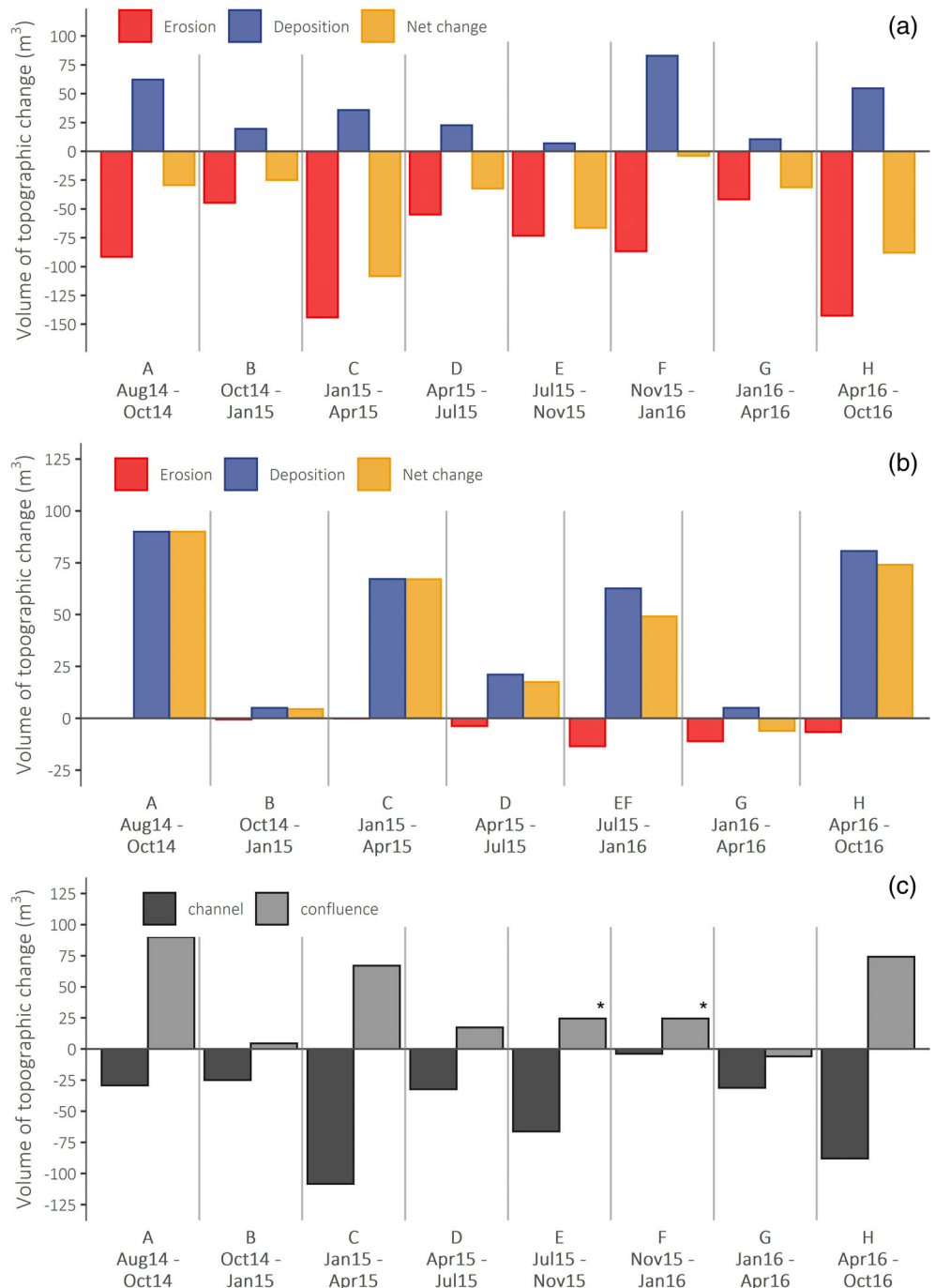
FIGURE 6 Volumes of topographic change: (a) in Ben Gill channel and (b) at the confluence. No data are available for periods E and F at the confluence bar. Instead, changes captured between E and F are pooled together (labelled "EF"). (c) Total volume of topographic changes in Ben Gill channel and the confluence. *Volume of change from DoD EF (confluence bar) was divided equally between E and F [Colour figure can be viewed at wileyonlinelibrary.com]

confluence (Figure 6c); rather, some material was progressively conveyed down the main-stem Ehen. Period A was the only time over which the net volume exported from Ben Gill was lower than deposition at the confluence (*c.* 90 m³, Figure 6c). Although this could be related to the "snapshot" nature of geomorphic change detection, or a large input of sediment from upstream compensating for internal erosion after the channel was engineered, this reversal of the normal pattern is considered to stem primarily from the coarse resolution of the baseline (GPS-based)
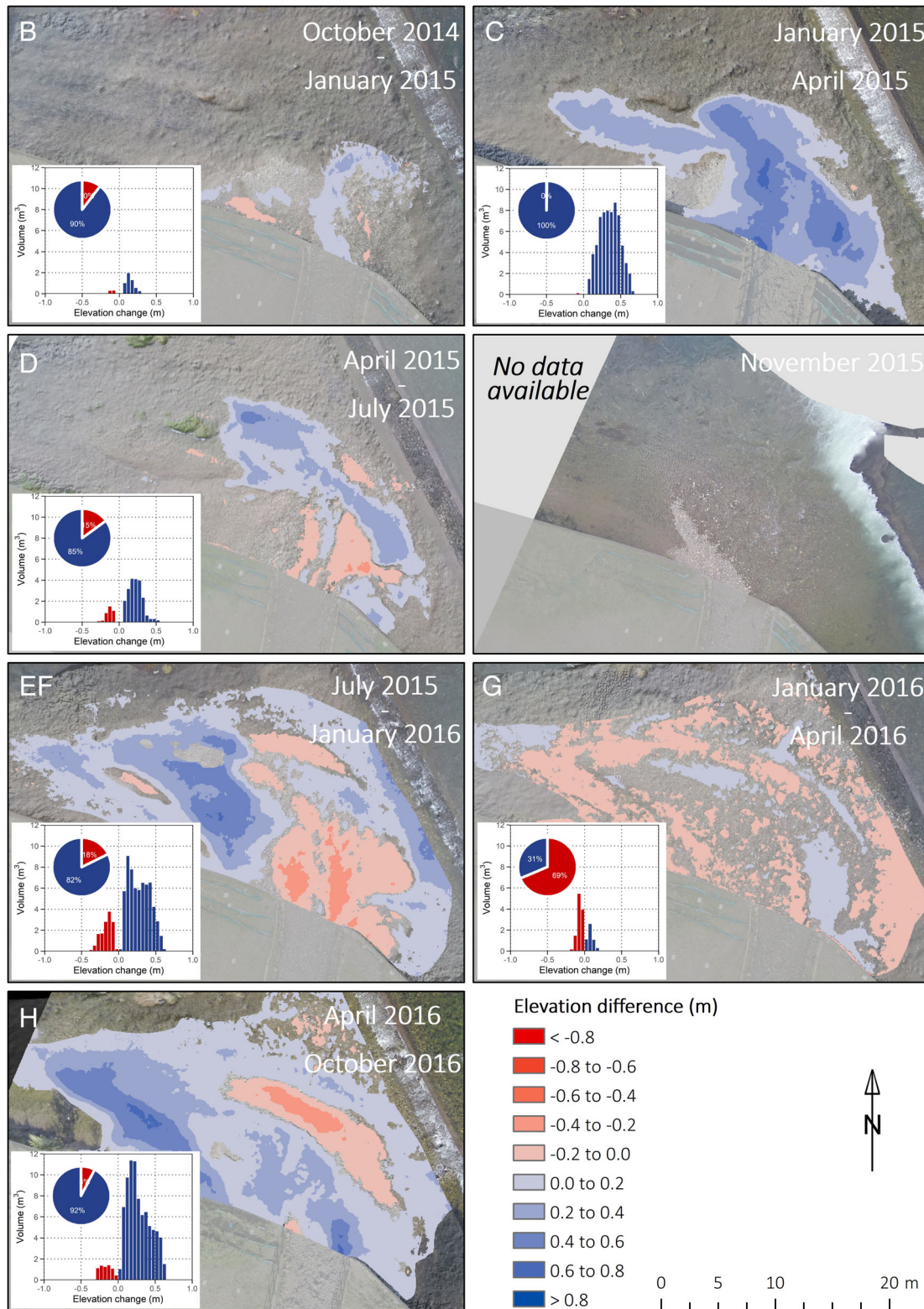
FIGURE 7 Topographic change (DoDs) and associated histograms for the confluence. No data was available for November 2015 at the confluence bar. Instead, the DoD was constructed as an "EF" period (i.e., between July 2015 and January 2016). See Section 3.2. for more details [Colour figure can be viewed at wileyonlinelibrary.com]

FIGURE 8 Evolution of particle size statistics of the confluence bar throughout the study. Error bars show 95% confidence intervals
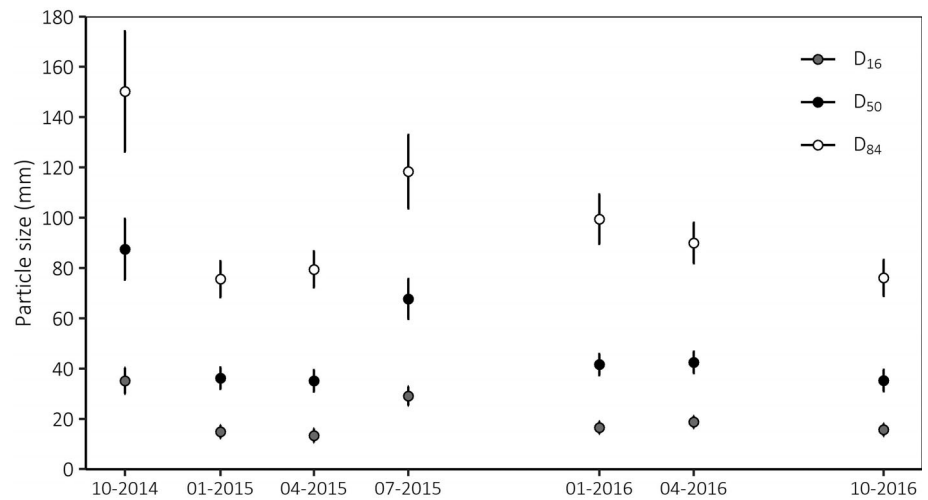
survey, especially because much visible erosion was observed following the extremely high flow on the first day after reconnection.

The confluence bar grew in size (i.e., continual positive geomorphic change) at a rate which has likely been underestimated due to issues related to detection of changes underwater. Comparing the total export of material from Ben Gill (c. 384 ± 65 m³) and the total storage at the confluence (c. 296 ± 28.6 m³), minimum volume of sediment effectively available in the Ehen can be estimated conservatively at around 88 m³ (c. 23% of the material supplied by Ben Gill).

It is worth stressing that the growth in size of the confluence bar tells only part of the story of material newly available to the Ehen, since some sediment may have been conveyed directly from Ben Gill to the main-stem without being deposited on the bar (and hence not quantified in the bar DoDs).

4.3.2 | Surface particle sizes

Median particle size on the bar was greatest during the first weeks following the reconnection (D_{50} = 87 ± 12 mm, Figure 8). As erosion continued in Ben Gill, the bar was covered with smaller particles and the D_{50} decreased rapidly. It remained consistently between 35 ± 4.3 mm and 42 ± 4.3 mm throughout the remainder of study, apart from the survey of July 2015 where all statistics (D_{16}, D_{50} and D_{84}) increased to higher values (e.g., D_{50} = 68 ± 8 mm). This July survey was also the first time that some erosion was observed on the bar, and it is likely that smaller particles deposited on the surface were washed away during the period between April and July 2015, leaving coarser particles exposed.

5 | DISCUSSION

5.1 | Bed material fluxes from Ben Gill

Results of the SfM photogrammetry suggest that Ben Gill exported sediment at an estimated minimum rate of ∼192 m³ y⁻¹ between

October 2014 and October 2016. Considering that virtually no coarse material was delivered to the upper Ehen for over 50 years, this represents a significant improvement. This estimated minimum volume is approximately twice the volume that was estimated from the (limited) available evidence prior to the reconnection (Brown et al., 2008). Erosion was still the dominant process observed in the newly constructed channel 2 years after its reconnection to the Ehen. Different mechanisms of adjustment in the newly constructed channel can be inferred from the spatial patterns of erosion and erosion magnitude. Patterns were not constant through time, as indicated by the shape of the frequency distribution of erosion (Figure 5). High magnitude changes are interpreted as being driven mainly by bank erosion, with the bottom of the bed assumed to still experience local degradation; this bed process is of lower magnitude but extends over larger areas than the bank erosion. Although part of the eroded material is fine particles (Marteau et al., 2018; Marteau, Batalla, et al., 2017), the development of a bar of gravel-sized material at the confluence shows that it includes coarser sediment. Erosional processes were evident following the rainfall event that coincided with the completion of the new channel, which proved to be the highest 24 hr precipitation ever recorded at the local weather station. In addition to the large release of fine sediment transported in suspension during the flows associated with this rainfall event (>35 t, 14% of the annual load; Marteau, Vericat, et al., 2017), a minimum of 90 m³ of coarse material was deposited at the confluence, eroded from the new Ben Gill channel, and/or potentially transferred from its upper catchment.

A higher internal reworking of sediment in Ben Gill was identified for period F, with larger volumes of deposition compared to other periods. This could be related to the regular rainfall events generated by the two successive storms of winter 2015, during which a total of 25 short (mean duration = 0.8 days) but intense flow events were recorded. As Ben Gill is not gauged, no data are available that might be used to statistically assess relations between flow magnitude, duration and frequency, and the geomorphic changes in the new channel. Even with discharge data, assessing these relations is a contentious subject (see summary by Dollar, 2002) and in the present

case is complicated by the fact that the channel is not (yet) in equilibrium.

The morphological budgeting approach used to produce estimates of sediment delivery to the confluence has some well-known limitations. The static nature of the method, used to capture a dynamic process, only offers a lower bound estimate of flux since there is no accounting for sediment transfer (Ashmore & Church, 1998). Compensating phenomena of scour and fill, which depend partially on the variable sediment supply from upstream and the number of competent events occurring between two surveys, cannot be fully captured by this budgeting approach (Lindsay & Ashmore, 2002). Nevertheless, it allows geomorphologists to make the most of high quality and density topographic data, with uncertainties and limitations that are not necessarily greater than other methods (Vericat, Wheaton, & Brasington, 2017).

Raw and thresholded values for net volume changes can be compared to see how bed material estimates are affected by the method used to assess errors, as recently discussed by Anderson (2019). Raw and thresholded values were rather similar for both Ben Gill channel (raw = −424.7 m^3, thresholded = −383.9 m^3) and the confluence bar (raw = +303.9 m^3, thresholded = +296.1 m^3, Table S1), showing that in the present case, given the length of the study reach and the magnitude of changes, the use of a more comprehensive approach to assess and propagate different types of errors only had an approximately 6% impact on overall net change estimates (Table S1).

5.2 | The confluence bar as a sediment buffer

Field observations and SfM analyses indicated that very little erosion of the confluence bar occurred during the first 2 years after the reconnection (total erosion = 11.2% of changes at the confluence); this is despite the high flows of winter 2015 (maximum discharge equivalent to 30-year return-period flood) and the evidence of fresh gravel deposits in the main-stem. This means that during the study period the Ehen was not capable of transporting all the coarse material delivered by the tributary. Because the confluence bar continues to grow, it is likely that the material identified as "exported" has had virtually no residence time in the bar. The behaviour of particles reaching the confluence can thus be described as binary: when a particle is eroded from Ben Gill and transferred to the confluence, it is either retained in the bar or transported directly to the main-stem. Particles that are deposited on the bar have limited chances of reaching the main-stem under ambient flow conditions, and hence remain until the next competent event. The bar can therefore be considered as buffer, mediating sediment processes occurring in Ben Gill and those in the Ehen.

This buffering effect of the confluence bar will continue until at least one of the factors controlling its growth and sediment entrainment changes. Of these, the main factor is the high sediment supply from Ben Gill. This is a very dynamic ephemeral headwater stream whose hydrologic and geomorphic activity contrast markedly with the regulated river Ehen. However, it is likely that its geomorphic activity

will stabilise in the future to some degree as it tends towards a quasi-equilibrium; adjustments in the slope and sinuosity of the newly created lower 300 m of channel will reduce local erosion and the system will mostly export material produced in the upper part of the catchment. Inherent features related to the old alluvial fan sedimentology may also play a role in this; for example, rocky outcrops may act as knick-points, cohesive material may prevent lateral erosion, and so forth. In fact, new knick-points were observed shortly after the first event, and these have migrated upstream as a function of regressive erosion (Figures S3 and S4) although their migration slowed down somewhat over the 2 year period. The time required to reach such equilibrium is difficult to assess, but a period of several years is likely.

The first flow event following completion of the new channel—associated with the extreme magnitude rainfall event of October 2014—deposited relatively large particles on the bar. Successive events delivered predominantly smaller particles, covering the bar as it continued to grow in size. Only the July 2015 survey saw the bar sediments increasing in size, with this considered as the first observation of proper local reworking of the bar (EF, Figure 7). Particle size has remained constant since this period, despite the occurrence of various erosion/deposition events. Ben Gill is capable of providing large clasts, so the size of material on the gravel bar reflects the transport capacity of the river Ehen. This capacity has been altered by the weir, but also by the proximity of the confluence bar to the weir. As visible in the aerial photographs (Figure 7), the bar now extends more or less all the way to the weir. As it is rather wide (60 m), the energy applied by the water when flow rises over the weir is dissipated over a large area. Additionally, now that the confluence bar has expanded, the distance available between the weir and the bar for the water to gain momentum is limited - when the water reaches the bar it has gained little kinetic energy and so has very limited competence. Thus, pace of sedimentary and geomorphic changes in the Ehen in the first period following the reconnection seems to be constrained more by transport capacity than sediment supply.

5.3 | Lessons for system-scale restoration

The present indirect (i.e. SfM) estimates of sediment exported from Ben Gill are at least twice as high as those anticipated from earlier studies (c. 100 m^3 per year, United Utilities, 2012). This difference reflects the high activity observed in the new and adjusting channel within the first 2 years following the reconnection. Practitioners are faced with several challenges and uncertainties when designing artificial gravel augmentation projects, related to logistical and economic issues as well as the geomorphic aspects of such work (Wheaton, Pasternack, & Merz, 2004). Channel conditions (geometry, slope, degree of armouring, grain-size distribution) as well as hydrological factors (availability of flows to mobilise newly added sediment) have to be taken into account in gravel augmentation projects (Pasternack, Wang, & Merz, 2004); moreover the volume of gravel to be injected, the grain-size distribution of this material, the timing and frequency of augmentation, and the location of the injection (Bunte, 2004;

Gaeuman, 2012) also have to be considered. Should the option of artificial gravel augmentation have been chosen for the Ehen instead of reconnecting the tributary, volumes of sediment injected would have been based on the preliminary estimates (United Utilities, 2012) and so would have been half the supply actually achieved by the reconnection to date. Artificial injection would also have required the construction of new vehicle access routes, with timing constrained by the fact that the river has several scenic and nature conservation designations (especially so as not to impact salmonid spawning and/or mussels at key life cycle stages).

As shown by the example of Ben Gill and the river Ehen, reconnecting affected reaches to their sediment source areas means that the volume and sizes of material, as well as the frequency and timing of supply, are controlled naturally by the system itself. As well as negating access and timing issues, the provision of material this way is likely to be sustained and so generate long-lasting geomorphological adjustments. Examples of this "system-scale" approach to river rehabilitation through the recovery of catchment connectivity pathways remain scarce, due to high initial costs, uncertainties related to achieving projects goals, lack of control, and public perception. Sediment connectivity is partially driven by the (geomorphic) history of a given system (Fuller, Riedler, Bell, Marden, & Glade, 2016). This, in turn, implies that actions taken to restore connectivity may change the course of local history. The extent of this change will depend on the scale of the processes that are restored.

To date, Ben Gill continues to supply large volumes of sediment, with the confluence bar acting as a buffer between this tributary and the Ehen. Although the new channel was designed to follow the original (pre-diversion) course of the stream, it will need time to reach a new "dynamic equilibrium," with changes in slope, channel geometry, sinuosity, bed configuration and sediment supply expected over the adjustment period. The continued supply of material offers the potential for improved mussel habitat in the river Ehen, though constrained by the fact that river remains regulated by the weir.

6 | FINAL REMARKS

Small sub-catchments can be significant sediment sources to main-stem systems (Rice, 1998). Ben Gill has proven to be a significant source of fine material (Marteau, Batalla, et al., 2017) and also exerts an important control on coarse sediment supply and dynamics. The geomorphic response of the upper Ehen to this renewed source of sediment is a function of both the nature of this source and that of the Ehen. As an important fraction of the material exported from Ben Gill remains stored at the confluence, the scale of the geomorphic response in the Ehen at present appears to be less than that of changes observed in Ben Gill. Nevertheless, some of the exported material is transferred downstream in the main-steam. The ability of the river to transport this material is key to achieving the overall goal of the restoration project, which is focussed on improving conditions for mussels in the main-stem Ehen. To some degree the system may be hydraulically limited because of the regulating effect of the lake on flows in the Ehen. This conclusion is supported by old aerial photographs which show a large confluence bar prior to the

diversion of Ben Gill. Restoring sediment connectivity is therefore only part of the project, and a key future element includes renaturalising flows by removing the weir. What is evident from the data presented here is that reconnecting the river Ehen with its small sub-catchment has been successful in restoring sediment supply to the main-stem in ways that would have been difficult to achieve through artificial augmentation.

DATA AVAILABILITY STATEMENT

The data that support the findings of this study are available from the corresponding author, BM, upon reasonable request.

ORCID

Baptiste Marteau https://orcid.org/0000-0002-5406-2907

REFERENCES

Abril, M., Muñoz, I., Casas-Ruiz, J. P., Gómez-Gener, L., Barceló, M., Oliva, F., & Menéndez, M. (2015). Effects of water flow regulation on ecosystem functioning in a Mediterranean river network assessed by wood decomposition. *Science of the Total Environment*, *517*, 57–65.

AgiSoft LLC. (2015). Agisoft PhotoScan Professional Edition. Version 1.2.3

Allan, J. D., & Castillo, M. M. (2007). *Stream ecology: Structure and function of running waters* (2nd ed.). Dordrecht, The Netherlands: Springer.

Alvarez-Codesal S, Sweeting RA. 2015. Historic changes in the Upper River Ehen Catchment. A Report for United Utilities. FBA unpublished report (S/0016/W).

Anderson, S. W. (2019). Uncertainty in quantitative analyses of topographic change: Error propagation and the role of thresholding. *Earth Surface Processes and Landforms*, *44*(5), 1015–1033. https://doi.org/10.1002/esp.4551

Arnaud, F., Piégay, H., Béal, D., Collery, P., Vaudor, L., & Rollet, A. J. (2017). Monitoring gravel augmentation in a large regulated river and implications for process-based restoration. *Earth Surface Processes and Landforms*, *42*(13), 2147–2166. https://doi.org/10.1002/esp.4161

Ashmore, P. E., & Church, M. A. (1998). Sediment transport and river morphology: A paradigm for study. In P. C. Klingeman, R. L. Beschta, P. D. Komar, & J. Bradley (Eds.), *Gravel-bed rivers in the environment* (pp. 115–163). Highland Ranch, CO: Water Resources Publications LLC.

Batalla, R. J., & Vericat, D. (2011). A review of sediment quantity issues: Examples from the river Ebro and adjacent basins (Northeastern Spain). *Integrated Environmental Assessment and Management*, *7*(2), 256–268. https://doi.org/10.1002/ieam.126

Boon, P. J. (1988). The impact of river regulation on invertebrate communities in the U.K. *Regulated Rivers: Research & Management*, *2*(3), 389–409. https://doi.org/10.1002/rrr.3450020314

Bracken, L. J., Turnbull, L., Wainwright, J., & Bogaart, P. (2015). Sediment connectivity: A framework for understanding sediment transfer at multiple scales. *Earth Surface Processes and Landforms*, *40*(2), 177–188. https://doi.org/10.1002/esp.3635

Brasington, J., Langham, J., & Rumsby, B. (2003). Methodological sensitivity of morphometric estimates of coarse fluvial sediment transport. *Geomorphology*, *53*(3–4), 299–316. https://doi.org/10.1016/S0169-555X(02)00320-3

Brasington, J., Rumsby, B. T., & McVey, R. A. (2000). Monitoring and modelling morphological change in a braided gravel-bed river using high resolution GPS-based survey. *Earth Surface Processes and Landforms*, *25*(9), 973–990. https://doi.org/10.1002/1096-9837

Brasington, J., Vericat, D., & Rychkov, I. (2012). Modeling river bed morphology, roughness, and surface sedimentology using high resolution terrestrial laser scanning. *Water Resources Research*, *48*(11), 1–18. https://doi.org/10.1029/2012WR012223

Brewer, P. A., & Passmore, D. G. (2002). Sediment budgeting techniques in gravel-bed rivers. In S. J. Jones & L. E. Frostick (Eds.), *Sediment flux to basins: Causes, controls and consequences* (pp. 97–113). London, England: Geological Society.

Brousse, G., Arnaud-Fassetta, G., Liébault, F., Bertrand, M., Melun, G., Loire, R., ... Borgniet, L. (2019). Channel response to sediment replenishment in a large gravel-bed river: The case of the Saint-Sauveur dam in the Buëch River (southern Alps, France). *River Research and Applications*, 1–14. https://doi.org/10.1002/rra.3527

Brown D, Butterill G, Bayliss B. 2008. Ben Ghyll Geomorphology report. Environment Agency, Version 2.0: Penrith, Cumbria

Buendía, C., Bussi, G., Tuset, J., Vericat, D., Sabater, S., Palau, A., & Batalla, R. J. (2016). Effects of afforestation on runoff and sediment load in an upland Mediterranean catchment. *Science of the Total Environment*, *540*, 144–157. https://doi.org/10.1016/j.scitotenv.2015.07.005

Bunte, K. (2004). *Gravel mitigation and augmentation below hydroelectric dams: A geomorphological perspective* (pp. 1–144). Fort Collins, CO: USDA Forest Service.

Church, M. (1995). Geomorphic response to river flow regulation—Case-studies and time-scales. *Regulated Rivers: Research & Management*, *11*(1), 3–22. https://doi.org/10.1002/rrr.3450110103

Csiki, S., & Rhoads, B. L. (2010). Hydraulic and geomorphological effects of run-of-river dams. *Progress in Physical Geography*, *34*(6), 755–780. https://doi.org/10.1177/0309133310369435

Dollar ESJ. 2002. Magnitude and frequency controlling fluvial sedimentary systems: Issues, contributions and challenges. IAHS-AISH Publication (276): 355–362.

Espa, P., Batalla, R. J., Brignoli, M. L., Crosa, G., Gentili, G., & Quadroni, S. (2019). Tackling reservoir siltation by controlled sediment flushing: Impact on downstream fauna and related management issues. *PLoS One*, *14*(6), 1–26. https://doi.org/10.1371/journal.pone.0218822

Ferguson, R. I., Cudden, J. R., Hoey, T. B., & Rice, S. P. (2006). River system discontinuities due to lateral inputs: Generic styles and controls. *Earth Surface Processes and Landforms*, *31*(9), 1149–1166. https://doi.org/10.1002/esp.1309

Foley, M. M., Bellmore, J. R., O'Connor, J. E., Duda, J. J., East, A. E., Grant, G. E., ... Wilcox, A. C. (2017). Dam removal—Listening in. *Water Resources Research*, *53*, 5229–5246. https://doi.org/10.1002/2017WR020457

Fryirs, K. (2013). (Dis)connectivity in catchment sediment cascades: A fresh look at the sediment delivery problem. *Earth Surface Processes and Landforms*, *38*(1), 30–46. https://doi.org/10.1002/esp.3242

Fuller, I. C., & Death, R. G. (2018). The science of connected ecosystems: What is the role of catchment-scale connectivity for healthy river ecology? *Land Degradation and Development*, *29*(5), 1413–1426. https://doi.org/10.1002/ldr.2903

Fuller, I. C., Large, A. R. G., Charlton, M. E., Heritage, G. L., & Milan, D. J. (2003). Reach-scale sediment transfers: An evaluation of two morphological budgeting approaches. *Earth Surface Processes and Landforms*, *28*(8), 889–903. https://doi.org/10.1002/esp.1011

Fuller, I. C., Riedler, R. A., Bell, R., Marden, M., & Glade, T. (2016). Landslide-driven erosion and slope-channel coupling in steep, forested terrain, Ruahine ranges, New Zealand, 1946-2011. *Catena*, *142*, 252–268. https://doi.org/10.1016/j.catena.2016.03.019

Gaeuman, D. (2012). Mitigating downstream effects of dams. In M. Church, P. M. Biron, & A. G. Roy (Eds.), *Gravel-bed rivers: Processes, tools, environments*. Chichester, England: John Wiley & Sons, Ltd..

Gibbins C, Young M, Hastie L, Soulsby C, Pokrajac D, Campbell L. 2004. River Ehen Freshwater Pearl Mussel Project: Final Report, Contract No. JB128. 44.

Gumpinger, C., Hauer, C., & Scheder, C. (2015). The current status and future challenges for the preservation and conservation of freshwater pearl mussel habitats. *Limnologica - Ecology and Management of Inland Waters*, *50*, 1–3. https://doi.org/10.1016/j.limno.2015.01.001

Habersack, H., & Piégay, H. (2008). River restoration in the Alps and their surroundings: Past experience and future challenges. In H. Habersack, H. Piégay, & M. Rinaldi (Eds.), *Gravel-bed rivers VI: From process understanding to river restoration* (pp. 703–735). Amsterdam: Elsevier.

Harvey B, McBain S, Reiser D, Rempel L, Sklar L. 2005. Key uncertainties in gravel augmentation: Geomorphological and biological research needs for Effective River restoration. Gravel Augmentation Report (April): 99.

Killeen I. 2006. The Freshwater Pearl Mussel, in the River Ehen Cumbria. Report on the 2006 Survey

Killeen I, Moorkens E. 2013. Environmental monitoring of the river Ehen freshwater pearl mussel population 2012: A report to united utilities. Malacological Services, Dublin

Killeen I, Oliver G. 1997. The freshwater pearl mussel (*Margaritifera margaritifera* [L. 1758]) in the river Ehen. Part 1. Report on 1996 Survey. 24.

Kondolf, G. M. (1994). Geomorphic and environmental effects of instream gravel mining. *Landscape and Urban Planning*, *28*(2–3), 225–243. https://doi.org/10.1016/0169-2046(94)90010-8

Kondolf, G. M. (1997). Hungry water: Effects of dams and gravel mining on river channels. *Environmental Management*, *21*(4), 533–551. https://doi.org/10.1007/s002679900048

Kondolf, G. M., Gao, Y., Annandale, G. W., Morris G regory, L., Jiang, E., Zhang, J., ... Yang, C. T. (2014). Sustainable sediment management in reservoirs and regulated rivers: Experiences from five continents. *Earth's Future*, *2*, 256–280. https://doi.org/10.1002/2013EF000184.of

Kondolf, G. M., Podolak, K., & Grantham, T. E. (2012). Restoring mediterranean-climate rivers. *Hydrobiologia*, *719*(1), 527–545. https://doi.org/10.1007/s10750-012-1363-y

Lallias-Tacon, S., Liébault, F., & Piégay, H. (2014). Step by step error assessment in braided river sediment budget using airborne LiDAR data. *Geomorphology*, *214*, 307–323. https://doi.org/10.1016/j.geomorph.2014.02.014

Lane, S. N. (2000). The measurement of river channel morphology using digital photogrammetry. *The Photogrammetric Record*, *16*(96), 937–961. https://doi.org/10.1111/0031-868X.00159

Lane, S. N., Westaway, R. M., & Hicks, D. M. (2003). Estimation of erosion and deposition volumes in a large, gravel-bed, braided river using synoptic remote sensing. *Earth Surface Processes and Landforms*, *28*(3), 249–271. https://doi.org/10.1002/esp.483

Lindsay, J. B., & Ashmore, P. E. (2002). The effects of survey frequency on estimates of scour and fill in braided river model. *Earth Surface Processes and Landforms*, *27*(1), 27–43. https://doi.org/10.1002/esp.282

López-Tarazón, J. A., Batalla, R. J., Vericat, D., & Francke, T. (2009). Suspended sediment transport in a highly erodible catchment: The river Isábena (southern Pyrenees). *Geomorphology*, *109*(3–4), 210–221. https://doi.org/10.1016/j.geomorph.2009.03.003

Marteau, B., Batalla, R. J., Vericat, D., & Gibbins, C. (2018). Asynchronicity of fine sediment supply and its effects on transport and storage in a regulated river. *Journal of Soils and Sediments*, *18*(7), 2614–2633. https://doi.org/10.1007/s11368-017-1911-1

Marteau, B., Batalla, R. J., Vericat, D., & Gibbins, C. N. (2017). The importance of a small ephemeral tributary for suspended sediment dynamics in a main-stem river. *River Research and Applications*, *33*, 1564–1574. https://doi.org/10.1002/rra.3177

Marteau, B., Gibbins, C. N., Vericat, D., & Batalla, R. J. (2020). Geomorphic response to system-scale rehabilitation: II. Mainstem channel adjustments following reconnection of an ephemeral tributary. *River Research and Applications* in press.

Marteau, B., Vericat, D., Gibbins, C., Batalla, R. J., & Green, D. R. (2017). Application of structure-from-motion photogrammetry to river restoration. *Earth Surface Processes and Landforms*, 42, 503–515. https://doi.org/10.1002/esp.4086

O'Leary D. 2013. Pearls in peril LIFE+ GB - action A3: Conservation actions for the freshwater pearl mussel in the river Ehen, Cumbria. 45.

Parker MS, Power ME. 1997. Effect of stream flow regulation and absence of scouring floods on trophic transfer of biomass to fish in northern California rivers. Technical report UCAL-WRC-W-825. Berkeley, CA

Pasternack, G. B., Wang, C. L., & Merz, J. E. (2004). Application of a 2D hydrodynamic model to design of reach-scale spawning gravel replenishment on the Mokelumne River, California. *River Research and Applications*, 20(2), 205–225. https://doi.org/10.1002/rra.748

Pearson, E., Smith, M. W., Klaar, M. J., & Brown, L. E. (2017). Can high resolution 3D topographic surveys provide reliable grain size estimates in gravel bed rivers? *Geomorphology*, 293(May), 143–155. https://doi.org/10.1016/j.geomorph.2017.05.015

Piqué, G., Batalla, R. J., & Sabater, S. (2016). Hydrological characterization of dammed rivers in the NW Mediterranean region. *Hydrological Processes*, 30(11), 1691–1707. https://doi.org/10.1002/hyp.10728

Pitlick, J., & Wilcock, P. (2001). Relations between streamflow, sediment transport, and aquatic habitat in regulated Rivers. *Water Science and Application*, 4, 185–198. https://doi.org/10.1029/WS004p0185

Ponsatí, L., Acuña, V., Aristi, I., Arroita, M., García-Berthou, E., von Schiller, D., … Sabater, S. (2015). Biofilm responses to flow regulation by dams in Mediterranean Rivers. *River Research and Applications*, 31(8), 1003–1016. https://doi.org/10.1002/rra.2807

Quinlan E. 2014. Ecogeomorphological dynamics of the river Ehen prior to its restoration. (PhD thesis). University of Aberdeen, Scotland

Quinlan, E., Gibbins, C. N., Batalla, R. J., & Vericat, D. (2015). Impacts of small scale flow regulation on sediment dynamics in an ecologically important Upland River. *Environmental Management*, 55, 671–686. https://doi.org/10.1007/s00267-014-0423-7

Quinlan, E., Gibbins, C. N., Malcolm, I., Batalla, R. J., Vericat, D., & Hastie, L. (2015). A review of the physical habitat requirements and research priorities needed to underpin conservation of the endangered freshwater pearl mussel *Margaritifera margaritifera*. *Aquatic Conservation: Marine and Freshwater Ecosystems*, 124, 107–124. https://doi.org/10.1002/aqc.2484

Rice, S. (1998). Which tributaries disrupt downstream fining along gravel-bed rivers? *Geomorphology*, 22(1), 39–56. https://doi.org/10.1016/S0169-555X(97)00052-4

Rice, S. P. (2017). Tributary connectivity, confluence aggradation and network biodiversity. *Geomorphology*, 277, 6–16. https://doi.org/10.1016/j.geomorph.2016.03.027

Sear, D. A. (1995). Morphological and sedimentological changes in a gravel-bed river following 12 years of flow regulation for hydropower. *Regulated Rivers: Research & Management*, 10(2–4), 247–264. https://doi.org/10.1002/rrr.3450100219

Smith, M. W. (2014). Roughness in the earth sciences. *Earth-Science Reviews*, 136, 202–225. https://doi.org/10.1016/j.earscirev.2014.05.016

Tena, A., Batalla, R. J., & Vericat, D. (2012). Reach-scale suspended sediment balance downstream from dams in a large Mediterranean river. *Hydrological Sciences Journal*, 57(5), 831–849. https://doi.org/10.1080/02626667.2012.681784

United Utilities. (2012). Hydrodynamic and Sediment Transport Modelling Report - Project Name: Ennerdale and Ben Gill - Project No: 80020012

Vázquez-Tarrío, D., Borgniet, L., Liébault, F., & Recking, A. (2017). Using UAS optical imagery and SfM photogrammetry to characterize the surface grain size of gravel bars in a braided river (Vénéon River, French Alps). *Geomorphology*, 285, 94–105. https://doi.org/10.1016/j.geomorph.2017.01.039

Vericat, D., Batalla, R. J., & Garcia, C. (2006). Breakup and reestablishment of the Armour layer in a large gravel-bed river below dams: The lower Ebro. *Geomorphology*, 76(1–2), 122–136. https://doi.org/10.1016/j.geomorph.2005.10.005

Vericat, D., Wheaton, J. M., & Brasington, J. (2017). Revisiting the morphological approach: Opportunities and challenges with repeat high resolution topography. In D. Tsustumi & J. B. Laronne (Eds.), *Gravel-bed rivers: Processes and disasters* (pp. 121–158). Tokyo, Japan: Wiley.

Westaway, R. M., Lane, S. N., & Hicks, D. M. (2000). The development of an automated correction procedure for digital photogrammetry for the study of wide, shallow, gravel-bed rivers. *Earth Surface Processes and Landforms*, 25, 209–226. https://doi.org/10.1002/(SICI)1096-9837

Westaway, R. M., Lane, S. N., & Hicks, M. D. (2001). Remote sensing of clear-water, shallow, gravel-bed Rivers using digital photogrammetry. *Photogrammetric Engineering & Remote Sensing*, 67(11), 1271–1281.

Wheaton, J. M., Brasington, J., Darby, S. E., & Sear, D. A. (2010). Accounting for uncertainty in DEMs from repeat topographic surveys: Improved sediment budgets. *Earth Surface Processes and Landforms*, 35, 136–156. https://doi.org/10.1002/esp.1886

Wheaton, J. M., Pasternack, G. B., & Merz, J. E. (2004). Spawning habitat rehabilitation-I. Conceptual approach and methods. *International Journal of River Basin Management*, 2(1), 3–20. https://doi.org/10.1080/15715124.2004.9635218

Williams GP, Wolman MG. 1984. Downstream effects of dams on alluvial rivers. U.S. Geological Survey Professional paper 1286: 94. DOI: https://doi.org/10.1126/science.277.5322.9j.

Wohl, E. (2017). Connectivity in rivers. *Progress in Physical Geography*, 41(3), 345–362. https://doi.org/10.1177/0309133317714972

Woodget, A. S., & Austrums, R. (2017). Subaerial gravel size measurement using topographic data derived from a UAV-SfM approach. *Earth Surface Processes and Landforms*, 42(9), 1434–1443. https://doi.org/10.1002/esp.4139

Woodget, A. S., Carbonneau, P. E., Visser, F., & Maddock, I. P. (2014). Quantifying submerged fluvial topography using hyperspatial resolution UAS imagery and structure from motion photogrammetry. *Earth Surface Processes and Landforms*, 64, 47–64. https://doi.org/10.1002/esp.3613

Wootton, J. T., Parker, M. S., & Power, M. E. (1996). Effects of disturbance on river food webs. *Science*, 273(5281), 1558–1561. https://doi.org/10.1126/science.273.5281.1558

Young, M. R., Cosgrove, P. J., & Hastie, L. C. (2001). The extent of, and causes for, the decline of a highly threatened naiad: *Margaritifera margaritifera*. In G. Bauer & K. Wächtler (Eds.), *Ecology and evolution of the freshwater mussels Unionoida* (Vol. 145, pp. 337–357). Berlin, Heidelberg: Springer.

SUPPORTING INFORMATION

Additional supporting information may be found online in the Supporting Information section at the end of this article.